JOURNAL OF VIROLOGY, Sept. 2007, p. 8996–9003 Vol. 81, No. 17
0022-538X/07/$08.00+0 doi:10.1128/JVI.00236-07

Retrograde Axonal Transport: a Major Transmission Route of Enterovirus 71 in Mice[▽]

Che-Szu Chen,[1]† Yi-Chuan Yao,[1]† Shin-Chao Lin,[1]† Yi-Ping Lee,[2] Ya-Fang Wang,[2] Jen-Ren Wang,[3] Ching-Chuan Liu,[4] Huan-Yao Lei,[1] and Chun-Keung Yu[1]*

Department of Microbiology and Immunology,[1] Institute of Basic Medical Sciences,[2] Department of Medical Laboratory Science and Biotechnology,[3] and Department of Pediatrics,[4] College of Medicine, National Cheng Kung University, Tainan, Taiwan, Republic of China

Received 4 February 2007/Accepted 5 June 2007

Inoculation of enterovirus 71 (EV71) by the oral (p.o.), intramuscular (i.m.), or intracranial route resulted in brain infection, flaccid paralysis, pulmonary dysfunction, and death of 7-day-old mice. The lag time of disease progression indicated that neuroinvasion from the inoculation sites was a prerequisite for the development of the clinical signs. Although EV71 p.o. inoculation led to a persistent viremia and a transient increase in blood-brain barrier permeability at the early stage of the infection, only low levels of virus, which led to neither severe infection nor clinical illness, could be detected in the brain, suggesting that hematogenous transport might not represent a major transmission route. In the spinal cord, following both p.o. and hind limb i.m. inoculation, the virus first appeared and increased rapidly in the lower segments, especially at the anterior horn areas, and then spread to the upper segments and brain in the presence of viremia. A reverse pattern, with the virus being first detected in the upper segment, was observed when the virus was i.m. inoculated in the forelimb. Colchicine, a fast axonal transport inhibitor, but not sciatic nerve transection reduced EV71 neuroinvasion in a dose-dependent manner, indicating a neuronal transmission of the virus.

Enterovirus 71 (EV71), a single-positive-stranded RNA virus that belongs to the *Enterovirus* genus of the *Picornaviridae* family, is a highly neurotropic virus and has been regarded as the most important neurotropic EV after the eradication of the poliovirus (11). The brain stem is most likely the major target of EV71 infection (2, 8). However, neither the host cell receptor nor the neurotransmission route of EV71 is fully defined.

As for poliovirus (PV), two possible routes by which the virus reaches the central nervous system (CNS) have been suggested: the virus either enters the CNS from the blood across the blood-brain barrier (BBB) or is transmitted to the CNS through peripheral nerves via retrograde axonal transport (1, 3, 14, 23). Expression of certain gene segments would be responsible for determining the capacity of PV to spread to the CNS through bloodstream or neuronal pathways (18).

In a cynomologus monkey model (12, 13), EV71 showed a wider-spread distribution pattern in the CNS than PV following both intracranial (i.c.) and intravenous inoculations, and monkeys exhibited extrapyramidal signs, including tremor and ataxia. However, after intraspinal inoculation, monkeys developed flaccid paralysis, a pyramidal sign suggesting direct virus invasion in the inoculation site. EV infection and persistence have been implicated in the pathogenesis of certain chronic muscle diseases (17). Furthermore, PV replicated in muscle cells that maintained constant viremia and spread to CNS from peripheral nerves (23). We previously showed that EV71 propagated more effectively in RD (human rhabdomyosarcoma) cells than in SK-N-SH (neuroblastoma) cells and Caco-2 (colorectal adenocarcinoma) cells. Furthermore, after oral (p.o.) inoculation of a mouse-adapted EV71 strain, EV71/MP4, 7-day-old ICR mice developed paralysis, with a mortality rate of 80%. Virus was first seen in the intestine. The virus then spread to muscle and CNS. A vast amount of virus was detected in the CNS and muscle, which led to neuronal loss and rhabdomyolysis of the mice with severe paralysis (21). In this study, we demonstrated that EV71 possesses strong neurotropism and that retrograde axonal transport in neuron cells might represent the major transmission route of EV71 in mice.

MATERIALS AND METHODS

Cells and virus. RD cells (American Type Culture Collection, Manassas, VA) were maintained in Dulbecco's modified Eagle's medium containing 10% fetal bovine serum plus 2 mM L-glutamine, 100 IU penicillin, and 100 μg of streptomycin per ml. EV71/MP4 strain, a mouse-adapted strain derived from parental virus EV71/Tainan/4643/98 (GenBank accession number AF304458) (22), was grown in RD cells. Working stocks contained 2×10^7 PFU/ml.

Experimental infection. Specific-pathogen-free, 7-day-old ICR mice (Laboratory Animal Center, National Cheng Kung University, College of Medicine, Tainan, Taiwan) were used. For i.c. inoculation, mice were injected with 10 μl of EV71/MP4 through the fontanelles using a 26-gauge needle. For intramuscular (i.m.) inoculation, 2-μl of the virus was injected into either the left hind limb or forelimb using a 26-gauge needle. For p.o. inoculation, mice were force fed with 200 μl of the virus using a 24-gauge feeding tube after fasting for 8 h. Control mice were given culture medium. Mice were observed twice daily for clinical signs and mortality for 2 weeks. Clinical disease was scored as follows: 0, healthy; 1, ruffled fur and hunchbacked appearance; 2, wasting; 3, limb weakness; 4, limb paralysis; and 5, moribund and death. To block virus transmission through nerves, colchicine (0.1 or 0.5 μg/2 μl/mouse; Sigma-Aldrich, St. Louis, MO), a fast axonal inhibitor, was injected into the left hind limb 12 h before viral inoculation. Limb weakness was the only side effect observed 24 h after the treatment, with gradual recovery within 1 week. The dose of colchicine that we used did not affect EV71 replication in vitro (data not shown). In other exper-

* Corresponding author. Mailing address: Department of Microbiology and Immunology, College of Medicine, National Cheng Kung University, Tainan, Taiwan 70101, Republic of China. Phone: 886-6-2353535, ext. 5673. Fax: 886-6-2082705. E-mail address: dckyu@mail.ncku.edu.tw.

† C.-S. Chen, Y.-C. Yao, and S.-C. Lin contributed equally to this study.

▽ Published ahead of print on 13 June 2007.

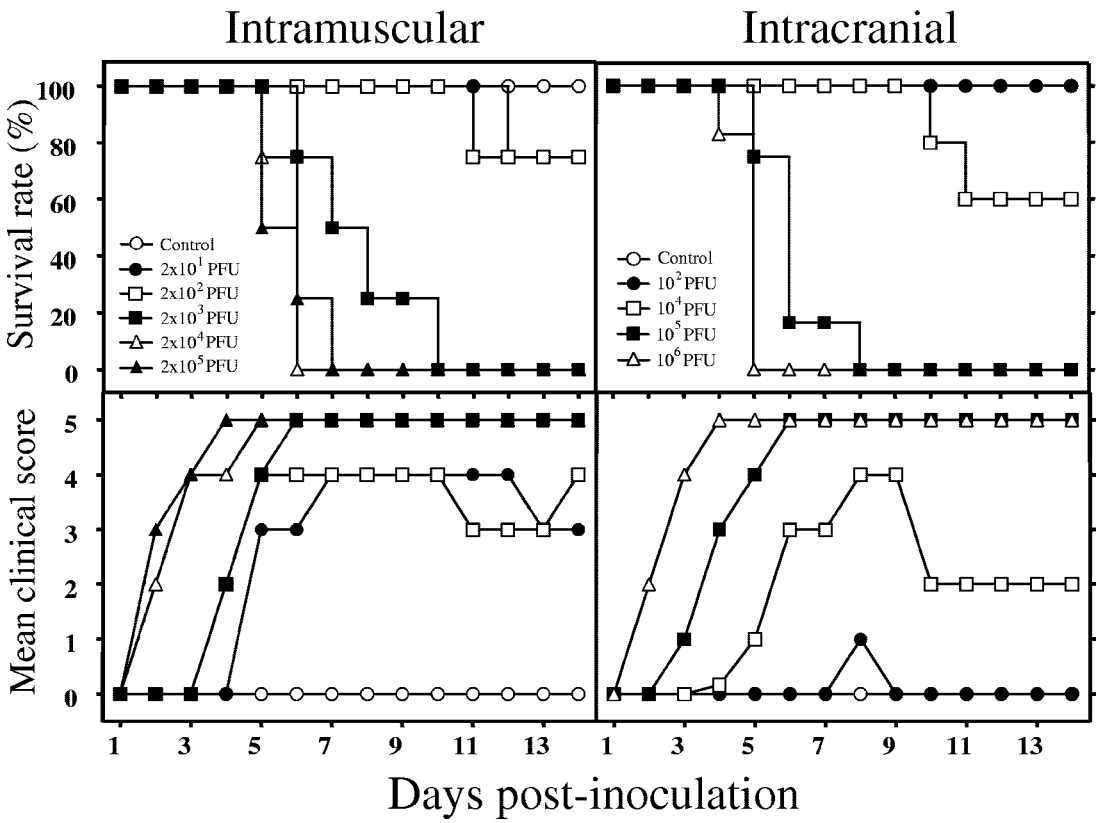

FIG. 1. i.m. and i.c. inoculation of EV71 result in dose-related paralysis and mortality. Seven-day-old ICR mice ($n = 12$) were i.m. (2×10^1 to 2×10^5 PFU/mouse; hind limb) or i.c. (10^2 to 10^6 PFU/mouse) inoculated with strain EV71/MP4. The survival rate was then monitored daily after infection. Clinical disease was scored as follows: 0, healthy; 1, ruffled hair, hunchbacked, or reduced mobility; 2, wasting; 3, limb weakness; 4, limb paralysis; and 5, death.

iments, the sciatic nerve of the left hind limb was dissected 24 h before infection. Sciatic nerve transection but not sham operation resulted in paresis of the left hind limb immediately after operation, indicating a complete blockade of the nerve. The institutional animal care and use committee approved all animal protocols.

Unrestrained whole-body plethysmograph. Airway responses of EV71-infected mice were measured in unrestrained animals using whole-body plethysmography (Buxco, Troy, NY). Readings were collected for 3 min after 3 min of resting in the chamber.

Evaluation of BBB permeability. Mice were intraperitoneally (i.p.) injected with poly(I:C) (Sigma-Aldrich) (20) or p.o. inoculated with EV71/MP4 as described above. Mice were then i.p. injected with 100 μl of 1% (wt/vol) Evans blue dye (Sigma-Aldrich) 1 h before sacrifice. After perfusion with isotonic saline containing EDTA, the whole brain was removed en bloc, weighed, and homogenized in *N*,*N*-dimethylformamide (Sigma-Aldrich). The optical density at 595 nm of the supernatant of the digested brain tissue was determined after incubation at 50°C for 72 h. For examination of Evans blue dye deposition, the perfused brains were immediately frozen in a liquid nitrogen-cold hexane bath in 100% OCT compound (Miles, Elkhart, IN). Cryosections (8 to 10 μm) (CM1800; Lecia, Wetzlar, Germany) were mounted on poly-L-lysine-coated slides, air dried, and fixed in cold acetone for 3 min. The sections were examined with a fluorescence microscope.

Sampling and tissue viral titer. For each experimental group, half of the animals (five or six mice) were subjected to virus detection, while the other half were subjected to histopathologic examination or immunohistochemical staining. After anesthetization with pentobarbital sodium (Nembutal; Abbott Laboratories, North Chicago, IL), blood samples were collected after axilla dissection. Tissue samples were aseptically removed, weighed, homogenized in 1 ml of Dulbecco's modified Eagle's medium, disrupted by three freeze-thaw cycles, and centrifuged after perfusion with isotonic saline containing EDTA. In other experiments, blood samples were pooled and red blood cells were removed with lysis buffer. Plasma and blood leukocytes were separated by centrifugation. All samples were stored at −70°C until assay. For viral titration, the samples were inoculated onto monolayers of RD cells and the cells were inspected daily for a minimum of 14 days for cytopathic effect (6). Viral titers were expressed as log PFU per mg of tissue or ml of blood. The lower limit of virus detection was 20 PFU.

Histopathology and immunohistochemical staining. Animals were perfused transcardially with isotonic saline followed by 4% paraformaldehyde. The cervical, thoracic, and abdominal cavities of mice were opened, and the tissues were immersion fixed in 10% buffered formalin for 48 h. Different parts of the brains and spinal cords were bisected, embedded in paraffin, and stained with hematoyxlin and eosin or Nissl stain. For viral staining, tissue sections were incubated with 0.3% H_2O_2 (10 min), MOM mouse immunoglobulin G blocking reagent (Vector Laboratories, Burlingame, CA) (1 h), anti-EV71 monoclonal antibody (MAb) (1:5,000 dilution; Chemicon) (2 h), and peroxidase-conjugated secondary Ab (1:7,500 dilution) (1 h) at room temperature. The sections were developed with aminoethyl carbazole (AEC substrate kit; Zymed, San Francisco, CA) and examined with a light microscope after counterstaining. Control sections were incubated with medium instead of MAb.

Reverse transcriptase PCR for EV71. RNA was extracted from leukocytes of infected mice (Trizol reagent; Invitrogen, Carlsbad, CA), and converted to cDNA with Moloney murine leukemia virus reverse transcriptase (Promega, Madison, WI). PCR amplification was performed on 4 μl of cDNA sample. Amplification cycle numbers and annealing temperatures were optimized for the specific primer pairs for the VP1 gene of EV71, 5′-GTGGCAGATGTGATTG AGAG-3′ and 5′-GTTATGTCTATGTCCCAGTT-3′. PCR products were electrophoresed on 2% agarose gels.

Statistics. The clinical scores and viral titer values were analyzed using either the nonparametric one-way analysis of variance or unpaired *t* test, and survival rates were analyzed by log rank analysis. The results are expressed as means ± standard errors of the means (SEM). A P value of <0.05 was considered significant.

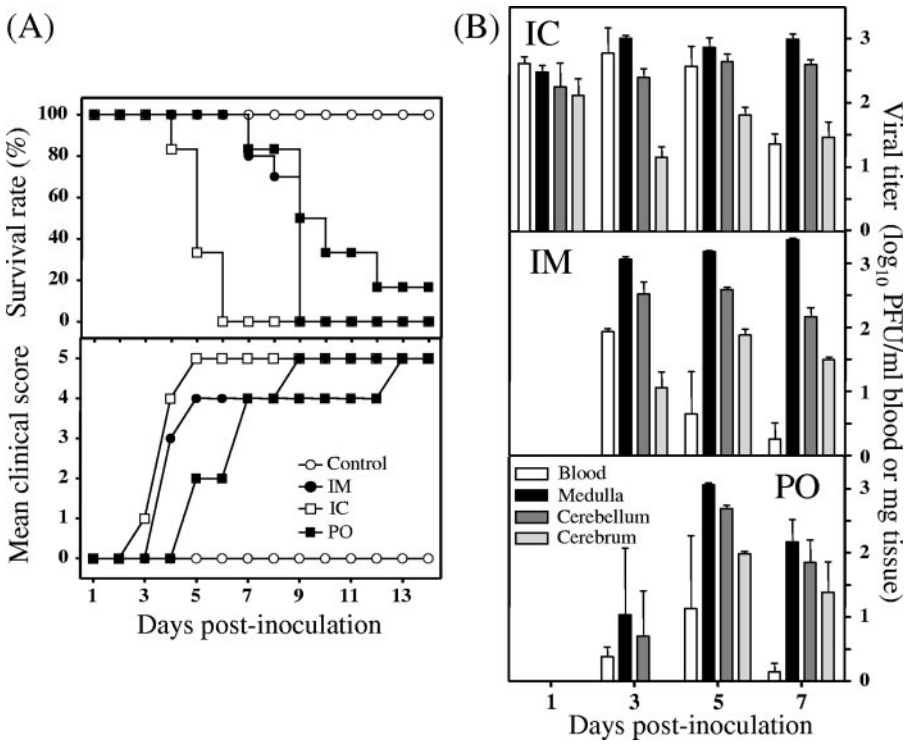

FIG. 2. The inoculation route determines the disease progression of EV71-infected mice. ICR mice ($n = 12$) were i.c., i.m. (hind limb), or p.o. inoculated with strain EV71/MP4 at 5×10^4, 5×10^3, and 5×10^6 PFU/mouse, respectively. Survival rate and clinical disease (A), and tissue viral load (B) were determined after infection. Results are the means and SEM.

RESULTS

Inoculation routes determine disease progression and rate of viral transmission to brain tissue of EV71-infected mice. Similar to the case for p.o. inoculation as we reported previously (21), both i.m. (2×10^1 to 2×10^5 PFU/mouse, left hind limb) and i.c. (10^2 to 10^6 PFU/mouse) inoculation of EV71 into 7-day-old ICR mice resulted in a dose-related flaccid paralysis and mortality (Fig. 1). The 50% lethal doses (LD_{50}) for i.m. and i.c. inoculations were 9.4×10^2 and 1.25×10^4 PFU/mouse, respectively, which were much lower than that for p.o. inoculation (5×10^6 PFU/mouse; 70 to 80% mortality). In experiments in which three groups of mice in parallel were inoculated with five times the LD_{50} of EV71 by the i.m or i.c. route or with the maximal lethal dose by the p.o. route, we observed that the disease progression in the infected mice was related to the inoculation routes. Specifically, mice inoculated by the i.c. route died earlier (4 to 6 days postinoculation [p.i.]) than those inoculated by the i.m. (7 to 9 days p.i.) or p.o. (>7 days p.i.) route (Fig. 2A). Clinically, i.c. inoculated mice developed initial flaccid paralysis in both the forelimbs and hind limbs and progressed rapidly to death (end point) within 1 to 2 days. On the other hand, i.m. and p.o. inoculated mice developed flaccid paralysis almost always in the hind limbs, with a longer lag time between the onset of the initial paralysis and death, which were at 3 to 4 days and >5 days p.i., respectively. High EV71 titers were detected in the brain tissue right after i.c. inoculation and were sustained for at least 7 days. However, following both i.m. and p.o. inoculations, the virus did not appear in brain tissue until day 3 p.i. The brain stem appeared to be the major replication site for EV71, as the viral titer in this area was 1 to 1.5 log units higher than those in the cerebellum and cerebrum regardless of the inoculation route (Fig. 2B).

EV71 infection induces pulmonary dysfunction. Whole-body plethysmograph analysis indicated that the pulmonary function of EV71-infected mice was severely compromised (Fig. 3). Peak inspiratory flow and tidal volume were significantly decreased in infected mice compared to age-matched, mock-infected mice. Interestingly, the occurrence of the pulmonary dysfunction was also related to the inoculation route. Dysfunction developed more rapidly in i.c. inoculated mice (day 3 p.i.) than in i.m. and p.o. inoculated mice (days 5 and 7, respectively). Histopathologically, lung sections of diseased mice exhibited emphysema without evidence of pulmonary edema (Fig. 4D to F [only the results for i.c. inoculated mice are shown).

Neuroinvasion by EV71. To determine the transmission of EV71, we monitored the viral titers in blood, different regions of the spinal cords, and brain following EV71 inoculations. Viremic spread occurred as early as 24 h after p.o. inoculation and persisted for at least 5 days p.i. (Fig. 5, upper panel). Plaque assays showed that plasma contained a majority of the virus present in the blood samples (whole blood, 5.3×10^2 PFU/ml; plasma, 5×10^2 PFU/ml), whereas the viral titer in the leukocyte fraction was below the detection limit of the assay. However, leukocytes also supported viral replication, as the viral genome could be detected in these cells by PCR (Fig. 5). Neuroinvasion with a very low viral titer was first evident in

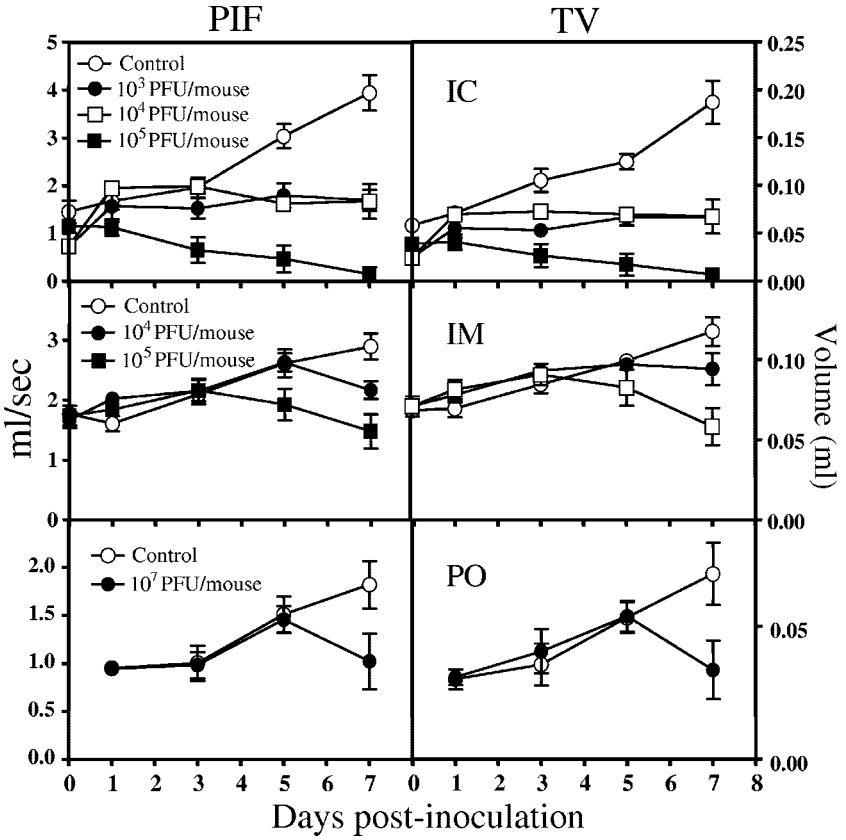

FIG. 3. The development of pulmonary dysfunction in EV71-infected mice is related to the inoculation routes. ICR mice (n = 12) were inoculated with EV71/MP4 i.c., i.m., or p.o. as described in the legend to Fig. 2. Peak inspiratory flow (PIF) and tidal volume (TV) were then monitored by whole-body plethysmography. Results are the means and SEM.

the medulla at 30 h p.i. Viral titer in brain tissue remained low (<10 PFU/mg tissue) within 48 h p.i. Virus was detected in the spinal cord at 48 h p.i., with a higher titer in the lower segments than in the upper segments and brain tissue (Fig. 5, lower panel). A similar pattern was observed following i.m. inoculation in the hind limb. At 24 h after i.m. inoculation, the virus was detected in the spinal cord, where the highest levels of replication occurred in the lumbar cord (Fig. 6A). In contrast, the reverse pattern of spread was observed with viral inoculation in the forelimb. The virus first appeared in the cervical cord at 24 h p.i., with a very small amount of virus detected in the other cords. Viral titers gradually increased, with the highest titer in the cervical cord, followed by the thoracic and lumbar cords. Virus was not detected in the brain until 48 h p.i.

EV71 can be detected in the spinal cord and brain stem with neuronal degeneration. Similar to the finding with p.o. inoculation (21), immunohistochemical staining using anti-EV71 VP1 protein MAb confirmed that the viral protein was present in the anterior horn regions of the lumbar cord as early as 6 h after i.m. inoculation in the hind limb, with a gradual increase in the numbers of positive-staining neurons from the lower to the upper spines over time (Fig. 6B). The localization of the viral antigen in the motor neurons of the anterior horn regions was consistent with the clinical manifestation of flaccid paralysis in the mice after i.m. inoculation in the hind limb. In the brain, EV71 antigen was mostly concentrated in the cerebellar peduncle of the brain stem underneath the cerebellum (Fig. 4A and B). Pathological changes, including neuropil vacuolation and myelin balls, developed in this area at later stages of the infection (day 5 p.i.) (Fig. 4C).

Colchicine but not sciatic nerve transection reduces EV71 spread from hind limb to CNS in mice. To investigate whether or not EV71 spread to the CNS from peripheral nerves, we either injected colchicine at 12 h or dissected the sciatic nerve of the left hind limb at 24 h before i.m. inoculation of EV71. Colchicine treatment reduced virus spread to the CNS in a dose-dependent manner. Viral titers in both the spine and brain were significantly lower ($P < 0.05$) in colchicine-treated mice than in phosphate-buffered saline (PBS)-treated control mice at 36 h p.i. (Fig. 7). A significant decrease in viral titers in the lumbar cord and brain was also observed at 48 h p.i. in the high-dose group. Although the transection slightly reduced the viral titers at the inoculation site (6 h p.i.) and in the spinal cord (24 h p.i.) early after inoculation, the differences were not statistically significant (data not shown).

EV71 induces BBB permeability. Since viremia was prominent before and after neuroinvasion, we monitored the BBB permeability in order to determine whether viremic spread through the BBB represented a route of neuroinvasion. We first demonstrated that poly(I:C) increased the BBB permeability in a dose-dependent manner which could be quantitated

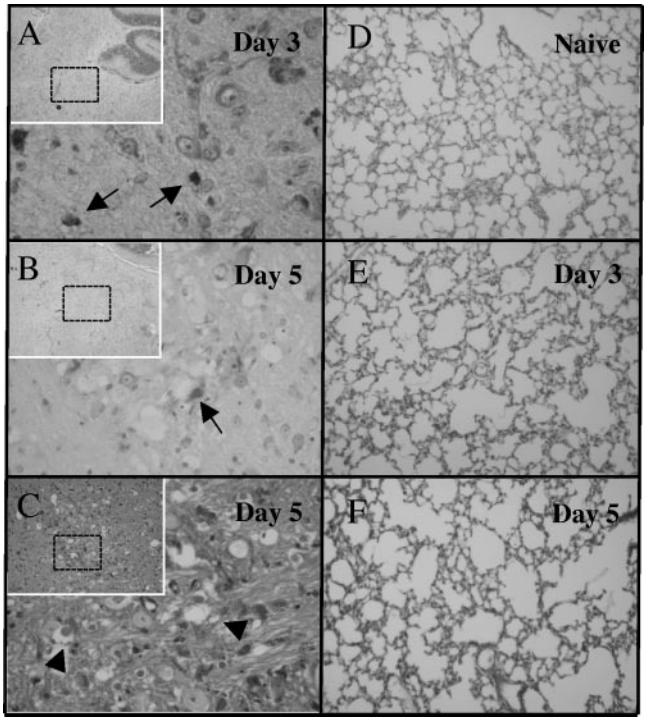

FIG. 4. i.c. EV71-inoculated mice develop brain lesions and emphysema at the late stage of infection. ICR mice were i.c. inoculated with EV71/MP4 (5×10^4 PFU/mouse). Brain and lung tissues were collected for general morphology (hematoyxlin and eosin stain) and immunohistochemical staining with anti-EV71 MAb. EV71 antigen (A and B, arrows) and neuropil vacuolation and myelin balls (C, arrowheads) occur in areas under the cerebellar peduncles. Magnifications, ×40 (insets in panels A, B, and C), ×200 (D, E, and F), and ×400 (A, B, and C).

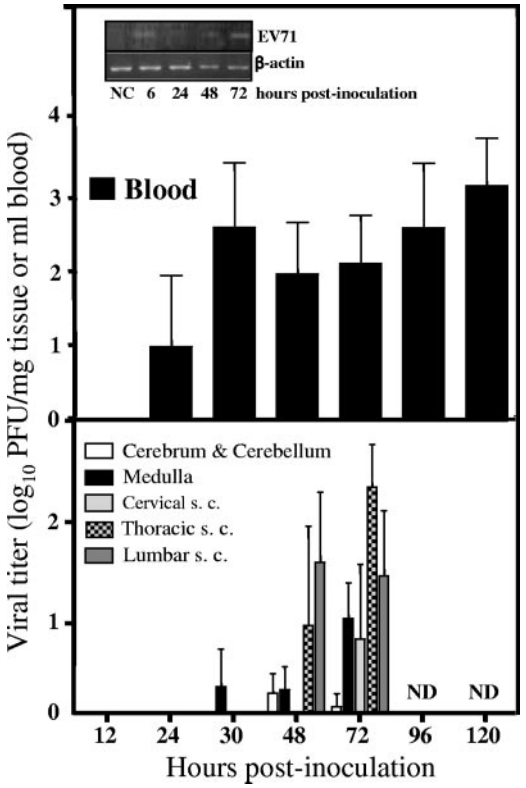

FIG. 5. p.o. EV71 inoculation results in viremia without severe neuroinvasion early after infection. ICR mice ($n = 12$ to 18) were p.o. inoculated with EV71/MP4 (5×10^6 PFU/mouse). The viral titers in the blood and CNS were determined by plaque assay. Results are the means and SEM. s. c., spinal cord; ND, not determined. Inset, detection of the EV71 genome in leukocytes. Agarose gel electrophoresis of the ethidium bromide-stained products of reverse transcriptase PCRs using RNA extracted from leukocytes of EV71-infected mice is shown. NC, sample without RNA.

by measuring the extravasation of Evans blue dye (Fig. 8A and B). The results showed that after p.o. inoculation of EV71, there was a transient increase in dye extravasation in the brain tissue as early as 30 h p.i. (Fig. 8C). Dye extravasations were further confirmed by the deposition of the characteristic red fluorescence of the dye around blood vessels in the meninges along the Zonula occludens (Fig. 8D). Coincidently, serum tumor necrosis factor alpha was slightly increased at 24 h p.i., and a marked increase was noted at 48 h p.i. (data not shown).

DISCUSSION

In our previous study (21), we demonstrated that EV71 replication was first and transiently detected in the small intestine following p.o. inoculation in mice. Viral replication was next observed in the spinal cord, especially the anterior horn regions, and then ascended to the brain. Thus, the pattern of the involvement of the spinal cord (a spread of the virus from the lower to upper segments) favors a retrograde axonal transport theory for EV71.

In this study, different inoculation routes and quantitation of tissue viral loads were applied to determine the transmission route of EV71 in mice. Regardless of the inoculation route, EV71 infection resulted in brain infection, paralysis, pulmonary dysfunction, and death. The i.c. inoculated mice displayed both forelimb and hind limb paralysis and demonstrated the shortest lag time to paralysis, lung dysfunction, and death. On the other hand, both p.o. and hind limb i.m. inoculated mice developed initial paralysis localized to the hind limbs, with a longer lag time to disease and mortality than that for i.c. inoculated mice. Furthermore, in mice with hind limb inoculation, the virus appeared to be spread from the lower to the upper spine. A reverse pattern, however, was seen in mice with forelimb inoculation. Thus, the time frame of the EV71-induced disease strongly indicated the transmission of the virus from the inoculation sites to the target tissues and that neuroinvasion was a prerequisite for its development. In addition, the pattern of paralysis and appearance of the virus in the CNS supported the hypothesis of axonal transport of the virus.

Colchicine treatment, which was effective in blocking fast axonal transport of PV in neuron cells (15), significantly reduced EV71 titers in the spinal cords and brain after i.m. inoculation. These data strongly indicated that retrograde axonal transport represents a transmission route of EV71 from the periphery to the CNS. Sciatic nerve block has been shown to prevent lethal challenge of PV in PV receptor transgenic mice (16) or to restrict the amount of virus in CNS (5). However, in our study, transection of the sciatic nerve was ineffec-

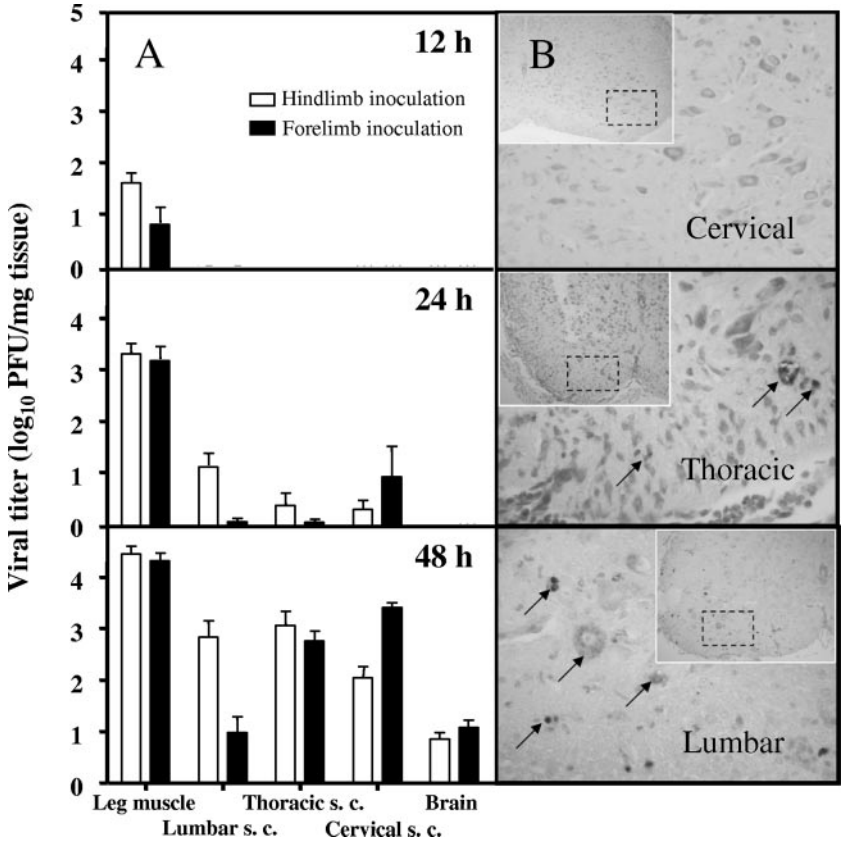

FIG. 6. EV71 neuroinvasion after i.m. inoculation. ICR mice (n = 6 to 12) were i.m. inoculated with EV71/MP4 (5×10^3 PFU/mouse) into either the left hind limb or forelimb. (A) The tissue viral titer was determined by plaque assay. Results are the means and SEM. s. c., spinal cord. (B) Presence of EV71 antigen in spinal cords. Sections of the spinal cords (48 h p.i. into hind limb) were stained with anti-EV71 MAb (arrows) and counterstained with Nissl stain. Note that the number of Nissl stain-positive neuronal cells was diminished in the anterior horn regions (insets).

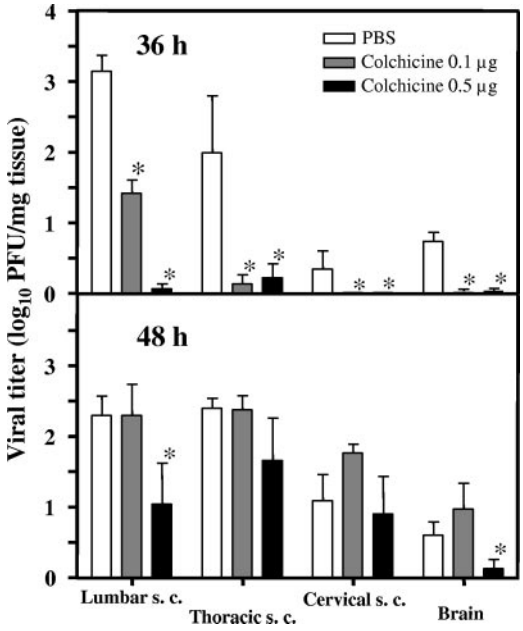

FIG. 7. Colchicine reduces EV71 spread to the CNS. ICR mice (n = 6 to 12) were i.m. inoculated with EV71/MP4 strain (5×10^3 PFU/mouse), with colchicine treatment (12 h before inoculation), in the hind limb. Control mice received PBS. The tissue viral titer was determined at 12, 24, 36, and 48 h after viral inoculation. Results are the means and SEM. *, $P < 0.05$ compared with PBS-treated mice. s. c., spinal cord.

tive for preventing EV71 dissemination. This was probably due to the rapid replication of EV71 in muscle and the presence of other termini of nerves in muscle whose pathway to the CNS was not blocked by sciatic nerve transection. Alternatively, the challenge dose may have been too high and might have produced an immediate viremia. It remains possible that the injection increased vascular permeability of the muscle to the virus, with a subsequent local spread into the spinal cord region that innervated the injected limb.

A steady viremia was constantly observed before and at the same times as detection of EV71 in the CNS. Therefore, the question of whether or not viremia was responsible for the transport of the viruses to the CNS arose. Persisting viremia may be the result of successful replication of EV71 in skeletal muscle, from which virus that shed into the bloodstream might invade the CNS through the BBB. Indeed, EV71 could trigger BBB opening accompanied by an augmentation of systemic and local tumor necrosis factor alpha production in the brain tissue, which might allow the entry of virus into the brain. We demonstrated that following p.o. inoculation, the natural infection route of EV71, there was a transient increase in BBB permeability as demonstrated by the extravascation and deposition of Evans blue dye in the brain tissue of infected mice at around 30 to 72 h p.i., a time frame in which the virus could be detected in the brain tissue. However, this early viral invasion

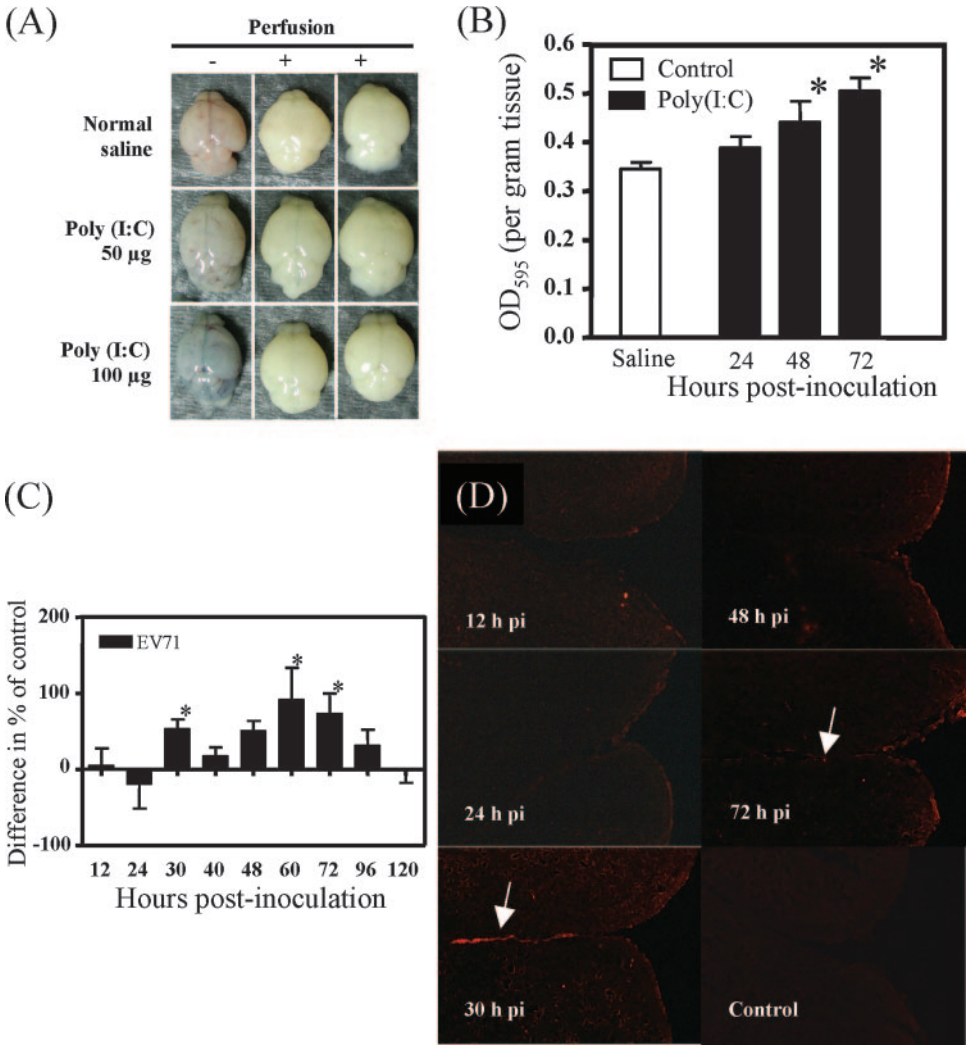

FIG. 8. Both poly(I:C) and EV71 induce an increase in BBB permeability. ICR mice ($n = 18$) were i.p. injected with poly(I:C) or p.o. inoculated with EV71/MP4 (5×10^6 PFU/mouse), and the increase in BBB permeability was determined by Evans blue dye extravasation. (A) Blue discoloration of brain tissue of poly(I:C)-treated mice at 48 h p.i. (B and C) Dye extravasation was quantified by measuring the OD at 595 nm of brain homogenates from poly(I:C)-treated mice (B) and EV71-inoculated mice (C) (mean OD for control, 0.463) after extraction. Results are the means and SEM. *, $P < 0.05$ compared with saline control. (D) The deposition of Evans blue dye in brain tissue (arrows) was examined in frozen sections using a fluorescence microscope. Magnification, ×100.

led to neither severe brain infection (low tissue titer), disease (low clinical score), nor a further viral transmission to the spinal cord. Thus, hematogenous transport might not represent a major transmission route of the virus. Concerning the vehicle for the virus, although the viral genome could be detected in leukocytes, the majority of the infectious virions in the blood samples were present in the plasma, indicating that infecting leukocytes was probably not the way by which the virus transported into the brain. Nevertheless, we cannot exclude the possibility that EV71 invaded the CNS by infecting the endothelial cells, as the virus could infect and activate human endothelial cells (7).

In this study we demonstrated that mice were remarkably more susceptible to i.m. inoculation of EV71 than to p.o. inoculation, with a surprising LD_{50} of 9×10^2 PFU, which was 1,000- and 100-fold lower than the LD_{50} for p.o. and i.c. inoculation, respectively. This may be explained by the fact that the virus bypassed the gut barrier and replicated more effectively in the muscle than in the gut. Skeletal muscle may host persistent EV71 infection (4) and become a vigorous viral source of entry into the bloodstream and the CNS. Similarly, both PV receptor transgenic mice (3) and wild-type mice (5) have been shown to be more susceptible to infection and paralysis after i.m. inoculation of PV.

Although EV71 infection exhibited brain stem damage and pulmonary dysfunction, we did not observe pulmonary edema, which is the most important phenotype of the EV71 infection in humans. The only obvious lesion seen in our animals was emphysema. Notably, the viral titer in the lung tissues remained low throughout the disease course. Thus, brain infection alone might not be sufficient for the development of pulmonary edema in mice. Other factors, such as cytokines or stress hormones, might be required (9, 10, 19).

The present work exposes the i.m. and i.c. routes, in addition

to the p.o. route, as routes of EV71 infection in mice. Following i.m. as well as p.o. inoculation, in spite of the fact that EV71 was present in many tissues as a result of viremia, EV71 replicated only in specific tissues, namely, muscle, spinal cord, and brain. Other extraneural tissues, including intestine, kidney, and liver, did not support EV71 replication, indicating that additional blocks to infection exist in these cell types. The muscle was likely involved in the subsequent neuroinvasion as the initial viral replication site. EV71 might spread from muscle to CNS through neuronal pathways as well as the bloodstream at certain times during infection. EV71 neuroinvasion resulted in paralysis, pulmonary dysfunction, and death of the animals. Well defining these infection models would accelerate our understanding of the pathogenesis of EV71.

ACKNOWLEDGMENT

This work was supported by National Research Program for Genomic Medicine grant NSC95-3112-B-006-007 from the National Science Council, Republic of China.

REFERENCES

1. **Bodian, D., T. Rivers, and F. Horsfall.** 1959. Viral and rickettsial infections of man, p. 479–498. Lippincott, Philadelphia, PA.
2. **Chen, C. Y., Y. C. Chang, C. C. Huang, C. C. Lui, K. W. Lee, and S. C. Huang.** 2001. Acute flaccid paralysis in infants and young children with enterovirus 71 infection: MR imaging findings and clinical correlates. Am. J. Neuroradiol. **22:**200–205.
3. **Crotty, S., L. Hix, L. J. Sigal, and R. Andino.** 2002. Poliovirus pathogenesis in a new poliovirus receptor transgenic mouse model: age-dependent paralysis and a mucosal route of infection. J. Gen. Virol. **83:**1707–1720.
4. **Douche-Aourik, F., W. Berlier, L. Feasson, T. Bourlet, R. Harrath, S. Omar, F. Grattard, C. Denis, and B. Pozzetto.** 2003. Detection of enterovirus in human skeletal muscle from patients with chronic inflammatory muscle disease or fibromyalgia and healthy subjects. J. Med. Virol. **71:**540–547.
5. **Ford, D. J., S. L. Ropka, G. H. Collins, and B. Jubelt.** 2002. The neuropathology observed in wild-type mice inoculated with human poliovirus mirrors human paralytic poliomyelitis. Microb. Pathog. **33:**97–107.
6. **Hsiung, G. D.** 1994. Virus assay, neutralization test and antiviral assay, p. 46–55. *In* G. D. Hsiung, C. K. Y. Fong, and M. L. Landry (ed.), Hsiung's diagnostic virology. Yale University Press, New Haven, CT.
7. **Liang, C. C., M. J. Sun, H. Y. Lei, S. H. Chen, C. K. Yu, C. C. Liu, J. R. Wang, and T. M. Yeh.** 2004. Human endothelial cell activation and apoptosis induced by enterovirus 71 infection. J. Med. Virol. **74:**597–603.
8. **Lin, T. Y., L. Y. Chang, S. H. Hsia, Y. C. Huang, C. H. Chiu, C. Hsueh, S. R. Shih, C. C. Liu, and M. H. Wu.** 2002. The 1998 enterovirus 71 outbreak in Taiwan: pathogenesis and management. Clin. Infect. Dis. **34**(Suppl. 2)**:**S52–S57.
9. **Lin, T. Y., L. Y. Chang, Y. C. Huang, K. H. Hsu, C. H. Chiu, and K. D. Yang.** 2002. Different proinflammatory reactions in fatal and non-fatal enterovirus 71 infections: implications for early recognition and therapy. Acta Paediatr. **91:**632–635.
10. **Lin, T. Y., S. H. Hsia, Y. C. Huang, C. T. Wu, and L. Y. Chang.** 2003. Proinflammatory cytokine reactions in enterovirus 71 infections of the central nervous system. Clin. Infect. Dis. **36:**269–274.
11. **McMinn, P. C.** 2002. An overview of the evolution of enterovirus 71 and its clinical and public health significance. FEMS Microbiol. Rev. **26:**91–107.
12. **Nagata, N., H. Shimizu, Y. Ami, Y. Tano, A. Harashima, Y. Suzaki, Y. Sato, T. Miyamura, T. Sata, and T. Iwasaki.** 2002. Pyramidal and extrapyramidal involvement in experimental infection of cynomolgus monkeys with enterovirus 71. J. Med. Virol. **67:**207–216.
13. **Nagata, N., T. Iwasaki, Y. Ami, Y. Tano, A. Harashima, Y. Suzaki, Y. Sato, H. Hasegawa, T. Sata, T. Miyamura, and H. Shimizu.** 2004. Differential localization of neurons susceptible to enterovirus 71 and poliovirus type 1 in the central nervous system of cynomolgus monkeys after intravenous inoculation. J. Gen. Virol. **85:**2981–2989.
14. **Ohka, S., N. Matsuda, K. Tohyama, T. Oda, M. Morikawa, S. Kuge, and A. Nomoto.** 2004. Receptor (CD155)-dependent endocytosis of poliovirus and retrograde axonal transport of the endosome. J. Virol. **78:**7186–7198.
15. **Ohka, S., W. X. Yang, E. Terada, K. Iwasaki, and A. Nomoto.** 1998. Retrograde transport of intact poliovirus through the axon via the fast transport system. Virology **250:**67–75.
16. **Ren, R., and V. R. Racaniello.** 1992. Poliovirus spreads from muscle to the central nervous system by neural pathways. J. Infect. Dis. **166:**747–752.
17. **Tam, P. E., and R. P. Messner.** 1999. Molecular mechanisms of coxsackievirus persistence in chronic inflammatory myopathy: viral RNA persists through formation of a double-stranded complex without associated genomic mutations or evolution. J. Virol. **73:**10113–10121.
18. **Tyler, K. L., D. A. McPhee, and B. N. Fields.** 1986. Distinct pathways of viral spread in the host determined by reovirus S1 gene segment. Science **233:**770–774.
19. **Wang, S. M., H. Y. Lei, K. J. Huang, J. M. Wu, J. R. Wang, C. K. Yu, I. J. Su, and C. C. Liu.** 2003. Pathogenesis of enterovirus 71 brainstem encephalitis in pediatric patients: roles of cytokines and cellular immune activation in patients with pulmonary edema. J. Infect. Dis. **188:**564–570.
20. **Wang, T., T. Town, L. Alexopoulou, J. F. Anderson, E. Fikrig, and R. A. Flavell.** 2004. Toll-like receptor 3 mediates West Nile virus entry into the brain causing lethal encephalitis. Nat. Med. **10:**1366–1373.
21. **Wang, Y. F., C. T. Chou, H. Y. Lei, C. C. Liu, S. M. Wang, J. J. Yan, I. J. Su, J. R. Wang, T. M. Yeh, S. H. Chen, and C. K. Yu.** 2004. A mouse-adapted enterovirus 71 strain causes neurological disease in mice after oral infection. J. Virol. **78:**7916–7924.
22. **Yan, J. J., I. J. Su, P. F. Chen, C. C. Liu, C. K. Yu, and J. R. Wang.** 2001. Complete genome analysis of enterovirus 71 isolated from an outbreak in Taiwan and rapid identification of enterovirus 71 and coxsackievirus A16 by RT-PCR. J. Med. Virol. **65:**331–339.
23. **Yang, W. X., T. Terasaki, K. Shiroki, S. Ohka, J. Aoki, S. Tanabe, T. Nomura, E. Terada, Y. Sugiyama, and A. Nomoto.** 1997. Efficient delivery of circulating poliovirus to the central nervous system independently of poliovirus receptor. Virology **229:**421–428.